VIRAL IMMUNOLOGY
Volume 26, Number 5, 2013

Pp. 322–335
DOI: 10.1089/vim.2013.0003

Crosstalk Between Autophagy and Apoptosis in RAW 264.7 Macrophages Infected With Ectromelia Orthopoxvirus

Lech Martyniszyn,[1] Lidia Szulc-Dąbrowska,[1] Anna Boratyńska-Jasińska,[1,3] Justyna Struzik,[1] Anna Winnicka,[2] and Marek Niemiałtowski[1]

Abstract

Several studies have provided evidence that complex relationships between autophagic and apoptotic cell death pathways occur in cancer and virus-infected cells. Previously, we demonstrated that infection of macrophages with Moscow strain of ectromelia virus (ECTV-MOS) induces apoptosis under *in vitro* and *in vivo* conditions. Here, we found that autophagy was induced in RAW 264.7 cells during infection with ECTV-MOS. Silencing of *beclin 1*, an autophagy-related gene, reduced the percentage of late apoptotic cells in virus-infected RAW 264.7 macrophages. Pharmacological modulation of autophagy by wortmannin (inhibitor) or rapamycin (inductor) did not affect or cause increased apoptosis in ECTV-MOS-infected RAW 264.7 cells, respectively. Meantime, blocking apoptosis by a pan-caspase inhibitor, Z-VAD-FMK, increased the formation of autophagosomes in infected macrophages. Taken together, three important points arise from our study. First, autophagy may co-occur with apoptosis in RAW 264.7 cells exposed to ECTV-MOS. Second, at later stages of infection, autophagy may partially participate in the execution of macrophage cell death by enhancing apoptosis. Third, when apoptosis is blocked infected macrophages undergo increased autophagy. Our results provide new information about the relationship between autophagy and apoptosis in ECTV-MOS-infected macrophages.

Introduction

Autophagy is a major process responsible for degradation of aggregated proteins and removal of damaged organelles in animal cells. During autophagy, double-membrane vesicles, termed autophagosomes, surround substrates for degradation and transport them to the lysosomes where they are digested. Autophagy (macroautophagy) is regulated by a network of autophagy-related (Atg) proteins that are responsible for autophagosome generation, elongation, maturation, and recycling. Atg proteins are divided into four functional groups, which are involved in regulation of autophagy at different stages (34). The first group, including a protein serine/threonine kinase complex (Atg1, Atg13, Atg17), regulates an early stage of autophagy by initiation of autophagosome formation and responds to upstream signals such as the target of rapamycin (TOR) kinase. The second group, containing a lipid kinase signaling complex (Atg6, Atg14, Vps34, and Vps15), mediates autophagosome nucleation that is driven by phosphatidylinositol (PI) phosphorylation (33,34). Beclin 1 (Bcl-2-interacting protein 1), which is a mammalian homolog of yeast Atg6/Vps30, is a key protein of the autophagy signaling pathway and participates in assembly of the PI-3-kinase class 3 (PI3KC3) complex during the early step of vesicle nucleation (28). The third group of Atg proteins involves two ubiquitin-like conjugation systems (the Atg8 and Atg12 systems) and is required for autophagosome expansion and completion. Microtubule-associated protein 1 light chain 3 (LC3) is the mammalian ortholog of yeast Atg8 that functions in the elongation of the phagophore membrane (54). The last group involves a retrieval pathway (Atg2, Atg9, and Atg18), which is required for disassembly of Atg proteins from matured autophagosomes (33,34).

Autophagy protects cells from different types of stress and does not necessarily induce cell death, but on the other side may contribute to cell death (type II programmed cell death, PCD II, referred to as autophagic cell death). The engagement of autophagy in cell death regulation is observed under physiological and pathophysiological conditions (34). Autophagic cell death is distinct from apoptosis (type I PCD)

Divisions of [1]Immunology, Department of Preclinical Sciences, and [2]Animal Pathophysiology, Department of Pathology and Veterinary Diagnostics, Faculty of Veterinary Medicine, Warsaw University of Life Sciences SGGW (WULS-SGGW), Warsaw, Poland.
[3]Molecular Biology Unit, Mossakowski Medical Research Centre, Polish Academy of Sciences, Warsaw, Poland.

and occurs independently of caspase activity and may be induced when apoptosis pathway is inhibited (13,57). In contrast to apoptosis, during autophagic cell death early degradation of cytoplasmic organelles and preservation of cytoskeletal elements until late stages are observed (34).

The functional relationship between autophagic and apoptotic pathways is complex, because both processes share common inducers, components, and can regulate the activity of each other (10,13,39). Depending on the cell type, stimulus and environmental conditions autophagy can support apoptosis in cell death induction or may assist apoptotic program without leading to cell death. On the other hand, autophagy may attenuate apoptosis and provide a protective mechanism from cell death execution (13).

A direct link between autophagy and apoptosis was recognized by common regulatory mechanisms shared by both pathways. It has been shown that several inducers of apoptosis such as etoposide, ceramide, or activation of the TRAIL receptor-2 can simultaneously activate autophagy (13). Further, reactive oxygen species (ROS) regulate both apoptosis and autophagy by favoring mitochondrial outer membrane permeabilization (MOMP) and inhibition of the cleavage activity of Atg4 during nutrient starvation, respectively (49). An increase in free cytosolic Ca^{2+} is a pro-apoptotic signal and is believed to induce autophagy through mammalian TOR (mTOR) inhibition (21). The best-known tumor suppressor, p53 transcription factor, reveals its anticancer properties by activation of apoptosis, but it also may promote cell survival by induction of autophagy (51). However, the most important common pathway regulating both processes depends on the Bcl-2 homology 3 (BH3) domain only proteins, which belong to the Bcl-2 family. Those proteins can interact *via* BH3 domain with the multidomain Bcl-2 family members and inhibit their anti-apoptotic (Bcl-2, Bcl-xL) or promote their pro-apoptotic (Bax, Bak) functions (39). Meanwhile, autophagy induction by Bcl-2 family members is based on their interactions with Beclin 1, another BH3-domain only protein. Beclin 1 reacts with anti-apoptotic Bcl-2 or Bcl-xL proteins, preventing the assembly of autophagosomes and ultimately inhibiting autophagy. BH3 mimetic compounds, such as (-)-gossypol, obatoclax, and ABT-737, as well as Bad, another BH3-only protein, completely disrupt the interactions of Beclin 1 with Bcl-2 or Bcl-xL, thus allowing the stimulation of autophagy (39,40).

Much of our current understanding of crosstalk between autophagy and apoptosis comes from studies on cancer cells, because targeting the mechanisms of cell death pathways in these cells creates new opportunities for the design of effective antitumor chemotherapeutics (2,6,36). Despite the increasing number of reports showing strategies of viruses to induce, inhibit, or modulate autophagic and apoptotic cell death pathways to benefit their survival (11,17,19,44,57), still the relationships between those two processes during viral infections are not fully understood.

Ectromelia virus (ECTV) causes a generalized infection, termed mousepox, in its natural host, the mouse. Together with variola virus (VARV), vaccinia virus (VACV), and cowpox virus (CPXV) belongs to the family *Poxviridae*, genus *Orthopoxvirus*. Mousepox model is used extensively to study viral immunology, genetic resistance to disease, and pathogenesis of smallpox and other generalized viral infections (5,9,38,41). Our previous investigations (9,30,41,42) have demonstrated that the virulent Moscow strain of ECTV (ECTV-MOS) induces apoptosis and autophagy in *in vitro* and *in vivo* conditions. Caspase-3- and caspase-7-dependent apoptosis was shown to regulate the resolution of ECTV-MOS infection (30). Induction of autophagy was demonstrated not to be required for the life-cycle of another orthopoxvirus—VACV (59). VACV replicated and maturated indistinguishably in the autophagy-deficient cell lines, the *atg5*$^{-/-}$ murine embryonic fibroblasts (MEFs) and the *beclin 1*$^{-/-}$ embryonic stem (ES) cells, as compared to in their isogenic wild-type (WT) counterpart cells (59).

The crosstalk between autophagy and apoptosis during ECTV-MOS infection has not yet been investigated and, therefore, the present study was undertaken with the aim of determining the above relationships. Because ECTV-MOS induces apoptosis in macrophages during late stages of infection (9), we first assessed the ability of ECTV-MOS to initiate autophagy in macrophages during its entire replication cycle. Second, we determined the effect of autophagy inhibitors or activators on ECTV-MOS-induced apoptosis in RAW 264.7 cells. And finally, we tested how modulation of apoptosis influences autophagy in ECTV-MOS-infected macrophages.

Materials and Methods

Cell culture

Mouse leukemic monocyte/macrophage RAW 264.7 (TIB-71) cell line was obtained from the American Type Culture Collection (Manassas, VA, USA). Cells were cultured in RPMI 1640 medium with Glutamax-I (Gibco BRL, Grand Island, NY, USA) supplemented with 10% fetal bovine serum (FBS; Sigma-Aldrich, St. Louis, MO, USA) and 1% antibiotic-antimycotic (100 U/mL penicillin, 100 μg/mL streptomycin, 250 ng/mL amfotericin-B) (Sigma-Aldrich) at 37°C in a humidified atmosphere with 5% CO_2 in air.

Virus

Highly infectious ECTV-MOS (ATCC 1374) was propagated and titrated by plaque-forming units (PFU) method in Vero cells (ATCC CCL-81). Virus stocks were stored in aliquots at −80°C until used. Infection of RAW 264.7 cells with ECTV-MOS was carried out at the multiplicity of infection (MOI) 5 in RPMI 1640 medium supplemented with 1% antibiotic-antimycotic (without FBS). After 45 min incubation at 37°C in a humidified 5% CO_2 atmosphere, medium was replaced by fresh culture medium supplemented with 2% FBS. After 2, 4, 6, 12, 18, and 24 hpi, cells were harvested for further experiments. Control cultures were identically processed but not infected with ECTV-MOS.

Pharmacological cell treatment

To inhibit autophagy, uninfected RAW 264.7 macrophages were treated for 2 h with wortmannin (wort; Sigma-Aldrich) at a final concentration of 0.1 μg/mL. To induce autophagy, cells were treated with 50 nM rapamycin (rapa; Sigma-Aldrich) for 30 min. For apoptosis inhibition, RAW 264.7 cells were exposed to a general caspase inhibitor N-benzyloxycarbonyl-Val-Ala-Asp-fluoromethyl ketone (Z-VAD-FMK) (Sigma-Aldrich) in a concentration of 20 μM.

siRNA knockdown of Beclin 1

Expression of Beclin 1 in RAW 264.7 macrophages was inhibited by BECN1 small interfering (si)RNA (Santa Cruz Biotechnology, Inc., Santa Cruz, CA, USA) according to the manufacturer's instructions. Briefly, 6 μL siRNA transfection reagent (Santa Cruz Biotechnology, Inc.) and 60 pmol siRNA were separately diluted in 100 μL siRNA transfection medium. The diluted siRNA solution was mixed with the diluted transfection reagent, incubated at room temperature for 30 min, and added to a 6-well plate seeded with 2×10^5 RAW 264.7 cells in 0.8 mL transfection medium. After 6 h, fresh culture medium containing 20% FBS was added and cells were incubated for an additional 18 h. Cells were infected with ECTV-MOS 24 h after transfection and collected at 18 hpi for immunoblot or flow cytometric analysis.

Protein preparation and Western blot analysis

RAW 264.7 cells were lysed using a mammalian cell lysis kit (MCL1; Sigma-Aldrich). Protein concentration of cell lysates was determined by bicinchoninic acid (BCA) assay (QuantiPRO BCA Assay Kit; Sigma-Aldrich) according to the manufacturer's instructions. Next, proteins were separated using sodium dodecyl sulfate polyacrylamide gel electrophoresis (SDS-PAGE). 12% or 15% polyacrylamide gels were used to resolve Beclin 1 (60 kDa) or LC3 (16 and 18 kDa), respectively. β-actin (42 kDa) was used as a protein loading control. After electrophoresis at 80 V for 2.5 h, protein bands were transferred onto polyvinylidene fluoride (PVDF) membrane at 70 V for 60 min in cold transfer buffer. The membranes were blocked for 1 h in 5% non-fat dry milk in TBST (Tris-buffered saline with Tween 20). After blocking, membranes were incubated with primary antibodies (Abs) overnight at 4°C as follows: rabbit anti-LC3 (1:1000; Sigma-Aldrich), rabbit anti-Beclin 1 (1:1000; Sigma-Aldrich), rabbit anti-ECTV-MOS (1:2000) (3), or mouse anti-β-actin (1:5000; Sigma-Aldrich). Next, membranes were rinsed in TBST and incubated for 1 h at room temperature with secondary Abs conjugated with horseradish peroxidase (HRP), goat anti-rabbit-HRP (1:50000; Sigma-Aldrich), or rabbit anti-mouse-HRP (1:50000; Sigma-Aldrich). The peroxidase activity was detected using chemiluminescent peroxidase substrate-1 (CPS-1; Sigma-Aldrich) according to the manufacturer's instructions, and then the membranes were exposed to X-ray film (Kodak, Rochester, NY, USA). Quantification of the bands from the immunoblots was performed using computerized densitometry (KODAK Image Station 4000MM Digital Imaging System, Rochester, NY, USA).

Immunofluorescent staining

Intracellular detection of proteins was performed with Cytofix/Cytoperm kit (BD Biosciences, San Jose, CA, USA) in accordance with the manufacturer's instructions. Briefly, control or ECTV-MOS-infected cells cultured on microscopic slides were fixed and permeabilized with Cytofix/Cytoperm (BD Biosciences) for 25 min on ice and then covered with 1% bovine serum albumin (BSA; Sigma-Aldrich) for 30 min. Next, slides were incubated for 1 h on ice with primary Abs (rabbit anti-LC3 or rabbit anti-Beclin 1) diluted 1:200 in Perm Wash solution (BD Biosciences). After washing, cells were incubated for 1 h on ice with goat anti-rabbit-FITC antibody (Sigma-Aldrich) diluted 1:500 in Perm Wash. In some experiments, ECTV-MOS antigens were stained intracellularly with rabbit polyclonal Abs conjugated with FITC, obtained as previously described (3). After staining, cells were post-fixed with 2% paraformaldehyde (PFA, Sigma-Aldrich) in phosphate-buffered saline (PBS). Nuclear or viral DNA were stained with 4',6'-diamidino-2-phenylindole (DAPI; Vector Labs, Burlingame, CA, USA). Imaging was performed using confocal microscope (Olympus FV1000, Tokyo, Japan) or fluorescence microscope (Olympus BX60) equipped with Color View III cooled CCD camera and Cell^F software (Olympus).

Autophagic vacuoles labeling with monodansylcadaverine (MDC)

RAW 264.7 cells grown on coverslips were incubated with 100 nM MDC (Sigma-Aldrich) in RPMI 1640 at 37°C for 1 h. After incubation, cells were washed three times with PBS, fixed with 2% PFA in PBS, and analyzed by Olympus BX60 fluorescence microscope using UV filter for DAPI (excitation filter: 330–385 nm, barrier filter: 420 nm).

Acidic compartments labeling with Lysotracker

Acidic compartments in control or ECTV-MOS-infected RAW 264.7 macrophages grown on coverslips were labeled with 1 μM Lysotracker Red (Invitrogen, Carlsbad, CA, USA) in PBS for 2 min at room temperature (RT). After washing with PBS, cells were fixed with 2% PFA in PBS. Cells were analyzed by Olympus BX60 fluorescence microscope using filters for rhodamine (excitation filter: 520–550 nm, barrier filter: 580 nm).

Apoptosis measurement by flow cytometry

Apoptosis was measured by Annexin V-FITC apoptosis detection kit (Sigma-Aldrich) according to the manufacturer's protocol. The percentage of apoptotic cells was determined using FACSCalibur flow cytometer equipped with CellQuest software (Becton-Dickinson, San Jose, CA, USA).

Statistical analysis

All quantitative data are expressed as mean ± SD from at least three independent experiments. Western blot experiments were analyzed using Mann-Whitney U test, and Student's t test was used for flow cytometric analysis. Significance was assessed at $p < 0.05$. All analyses were performed with Statistica 6.0 software (Statsoft Inc.,Tulsa, OK, USA).

Results

RAW 264.7 macrophages are permissive to ECTV-MOS infection

First, we assessed whether ectromelia virus is able to infect RAW 264.7 macrophages, which are typical antigen presenting cells (APCs). Cells were infected with ECTV-MOS at a multiplicity of 5 per cell. Such MOI infected at least 99% of cells in culture as predicted by the Poisson distribution (52). Duration of infection (18 hpi) was chosen on the basis of earlier studies of VACV, myxoma virus, and ECTV replication cycle. At this time point, virus-induced morphological and functional changes of cells are well observed (3,30). Viral proteins were detected in whole cell lysate by Western blot

assay. After 18 hpi in RAW 264.7 cells, the amount of viral proteins was at a comparable level to that observed in permissive L929 fibroblasts (Fig. 1a). In control uninfected RAW 264.7 and L929 cells, no viral proteins were detected. As revealed by fluorescence microscopy, at 18 hpi macrophages displayed changed morphology with long projections (Fig. 1b). Within the cytoplasm, many viral particles were detected by co-localization of pAb anti-ECTV-FITC and DAPI, which also binds to viral DNA (Fig. 1b).

Autophagy is induced in RAW 264.7 cells during ECTV-MOS replication cycle

Western blot assay was used to determine the expression of LC3-II and Beclin 1 in control and ECTV-MOS-infected RAW 264.7 macrophages. LC3 proteins were separated on 15% polyacrylamide gel to obtain LC3-I (18 kDa) and LC3-II (16 kDa) protein bands. Levels of LC3-II (autophagosomal marker) and Beclin 1 (60 kDa) were measured relative to β-actin (42 kDa) loading control. An increase in LC3-II protein level was observed during the whole replication of ECTV-MOS in RAW 264.7 cells starting from 2 hpi (Fig. 2a and 2b). Quantitative analysis of LC3-II relative to β-actin revealed 3-fold increase in LC3-II expression in cells as soon as 2 hpi with ECTV-MOS compared to control uninfected macrophages ($p = 0.009$). The highest increase in LC3-II expression was observed during later stages of ECTV-MOS replication: 7-fold ($p = 0.009$), 5.5-fold ($p = 0.009$), and 8-fold ($p = 0.009$) at 12, 18, and 24 hpi, respectively (Fig. 2b). The protein content of Beclin 1 remained unchanged in RAW 264.7 cells during the course of ECTV-MOS replication (Fig. 2a and 2b).

To support the data described in Figure 2a and 2b, we performed microscopic analysis of LC3-II distribution in RAW 264.7 macrophages infected with ECTV-MOS. At 18 hpi, distribution of LC3 protein changed within the cytoplasm—from diffuse localization to punctate aggregates,

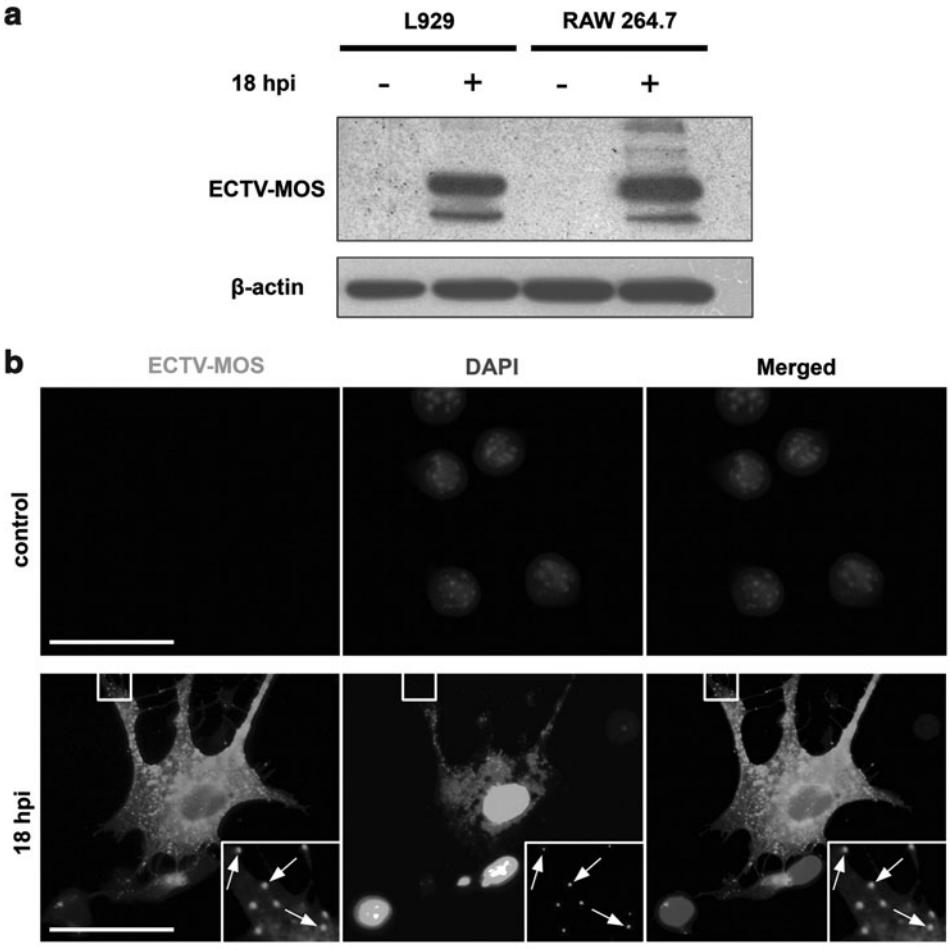

FIG. 1. Detection of ECTV-MOS antigens in cultured cells. **(a)** Western blot analysis of the viral protein content in mock-infected (control) or ECTV-MOS-infected L929 and RAW 264.7 cells at 18 hpi. Viral antigens were detected using primary rabbit pAbs against ECTV-MOS and secondary goat anti-rabbit Abs conjugated with HRP. Equal loading of protein extract was confirmed by β-actin. **(b)** Fluorescence microscopy analysis of virus distribution in mock-infected and ECTV-MOS-infected RAW 264.7 macrophages at 18 hpi. Uninfected RAW 264.7 cells stained for ECTV-MOS are shown as a specificity control. Virus-infected cells show co-localization of viral DNA stained by DAPI with ECTV-MOS antigens indicated by *arrows*. Analyses were performed using fluorescence microscope (Olympus BX60). Scale bars: 30 μm.

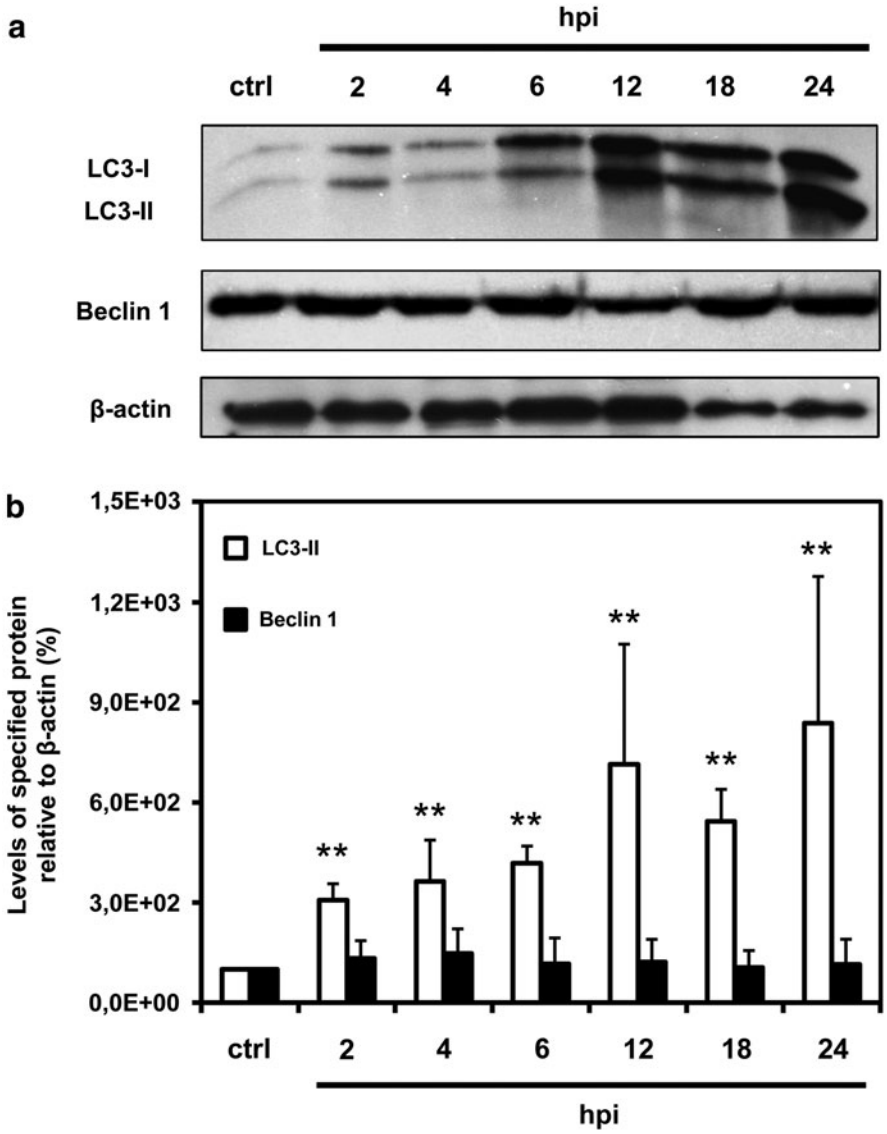

FIG. 2. Quantitative analysis of LC3-II and Beclin 1 expression in RAW 264.7 macrophages during ECTV-MOS replication cycle. **(a)** Representative Western blot analysis of LC3-I (18 kDa), LC3-II (16 kDa), Beclin 1 (60 kDa), and β-actin (42 kDa) expression in mock-infected (ctrl) and ECTV-MOS-infected cells at 2, 4, 6, 12, 18, and 24 hpi. **(b)** Quantitative measurement of LC3-II and Beclin 1 proteins in macrophages during ECTV-MOS infection. Amounts of proteins were normalized to β-actin (served as a control for protein loading) and are relative to amounts in control cells. The values are presented as mean ± SD from 4 to 5 independent experiments. Significant differences in LC3-II and Beclin 1 levels between control and ECTV-MOS-infected cells are shown by *asterisks* (Mann–Whitney U test, $*p < 0.05$, $**p < 0.01$ *vs* control).

what may correspond to the protein association with autophagosomal membranes (Fig. 3a). For microscopic analysis of autophagy we used fluorescent dyes that have affinity for acidic organelles. Within RAW 264.7 macrophages at 18 hpi with ECTV-MOS we observed an increase in accumulation of granular structures of high MDC fluorescence intensity (Fig. 3b) and Lysotracker-positive acidified vacuoles (Fig. 3c), compared to uninfected control cells.

Intracellular distribution of Beclin 1 in control and infected RAW 264.7 macrophages varied as revealed by fluorescence microscopy (Fig. 3d). The spatial distribution of Beclin 1 changed from a uniform intracellular distribution in uninfected cells to strongly co-localized with the extranuclear virus replication centers in infected RAW 264.7 cells (Fig. 3d). This result suggests that Beclin 1 may be involved in ECTV-MOS replication; however, further studies are needed to confirm this statement.

Decreased level of late apoptosis in beclin 1-knockdown RAW 264.7 cells infected with ECTV-MOS

To assess the role of autophagy in regulation of apoptosis and/or its interaction with type I cell death we impaired the

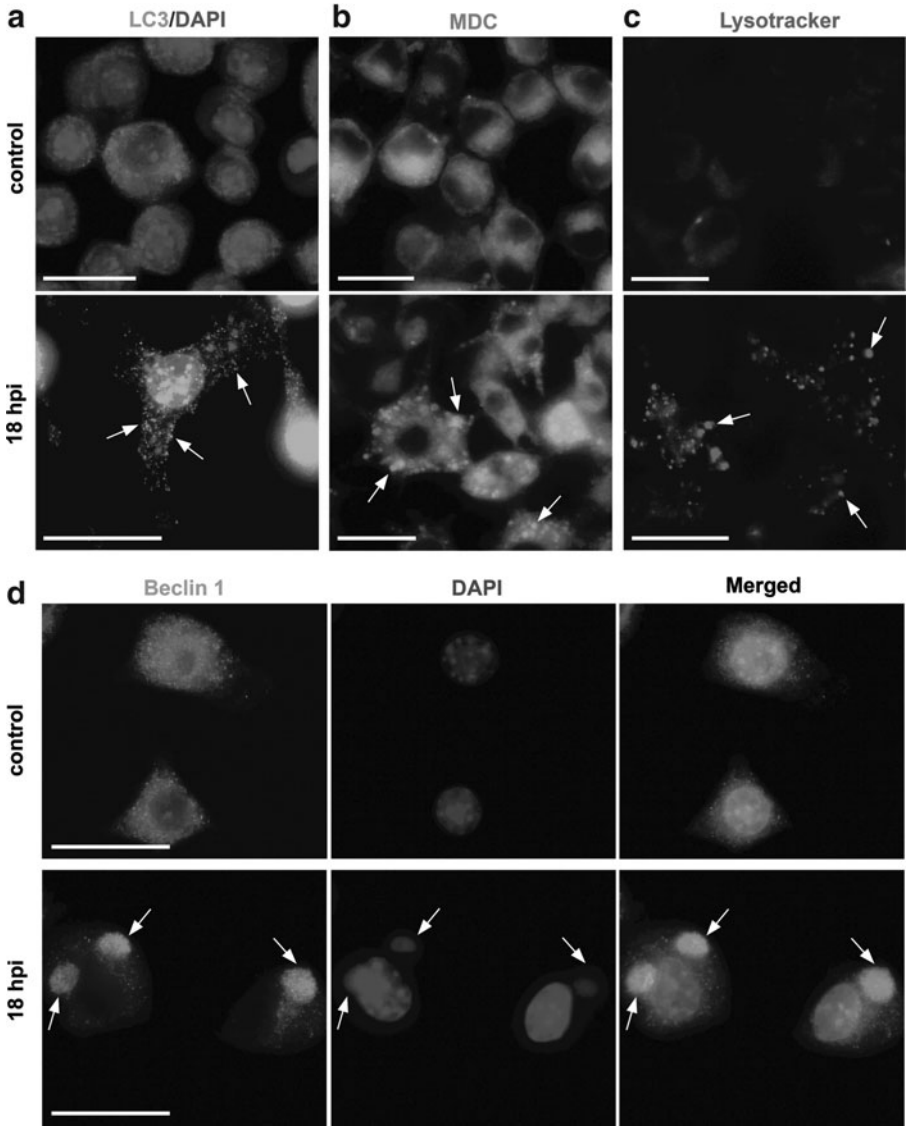

FIG. 3. Induction of autophagy in ECTV-MOS-infected RAW 264.7 macrophages. **(a)** Distribution of LC3 protein in mock-infected (control) and ECTV-MOS infected cells at 18 hpi. Punctate aggregates of LC3 protein are indicated by *arrows*. Cellular nuclei and viral DNA were counterstained by DAPI. **(b)** Increased formation of MDC-positive vesicular structures (*arrows*) in ECTV-MOS infected macrophages. Mock- or virus-infected RAW 264.7 cells at 18 hpi were treated with 100 nM MDC in culture medium for 1 h at 37°C and fixed with 2% PFA. **(c)** Generation of Lysotracker-positive acidified vacuoles (*arrows*) in ECTV-MOS-infected cells. Control and infected macrophages at 18 hpi were incubated with 1 μM Lysotracker Red in PBS for 2 min at RT and fixed with 2% PFA. **(d)** Beclin 1 and cellular nuclei and viral DNA distribution in uninfected and ECTV-MOS-infected RAW 264.7 cells at 18 hpi. The co-localization of Beclin 1 with viral DNA is indicated by *arrows*. All analyses were conducted under a fluorescence microscope (Olympus BX60). Scale bars: 30 μm.

autophagy process using RNA interference for *beclin 1*. Efficiency of *beclin 1* silencing was confirmed by Western blot analysis (Fig. 4a). Densitometric analysis of protein bands revealed that in RAW 264.7 cells *beclin 1*, siRNA reduced the Beclin 1 protein level by approximately 80% compared to untreated WT and control RNAi-treated RAW 264.7 cells (Fig. 4b). The percentage of early and late apoptotic cells was determined in uninfected control siRNA treated RAW 264.7 cells (ctrl-siRNA), RAW 264.7 macrophages with downregulation of Beclin 1 mediated by siRNA interference (siBecn 1), ECTV-MOS-infected control siRNA-transfected RAW 264.7 cells (ctrl-siRNA/ECTV), and ECTV-MOS-infected siBecn 1-transfected RAW 264.7 cells (siBecn 1/ECTV). Statistical analysis of the percentage of early apoptotic cells did not reveal any significant changes between ECTV-MOS-infected ctrl-siRNA at 18 hpi and uninfected ctrl-siRNA cells or ECTV-MOS-infected siBecn 1 cells and uninfected siBecn 1 cells (Fig. 4c). Meantime, the percentage of late apoptotic/necrotic cells significantly ($p = 0.0001$) increased in infected control and

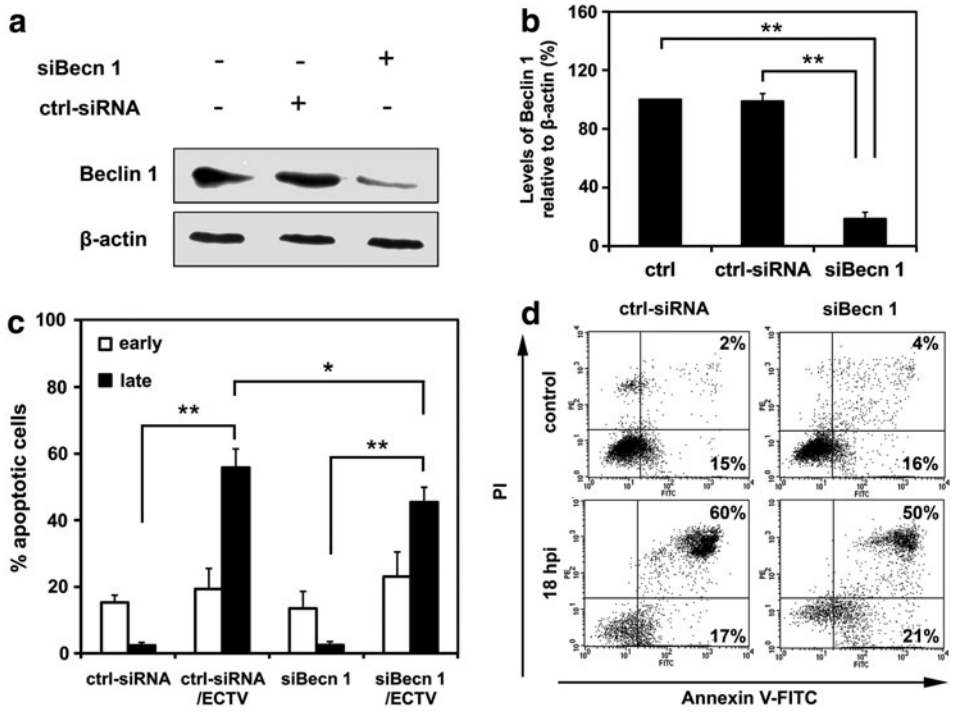

FIG. 4. Silencing of *beclin 1* by siRNA leads to reduced apoptosis level in ECTV-MOS-infected RAW 264.7 cells. **(a)** Western blot analysis of Beclin 1 (62 kDa) levels in untreated control cells (ctrl), control RNAi-treated cells (ctrl-siRNA), and *beclin 1*-silenced cells (siBecn 1). The *β*-actin (42 kDa) control was used to confirm equal loading of protein. **(b)** Quantitative measurement of Beclin 1 protein in ctrl, ctrl-siRNA, and siBecn 1 RAW 264.7 cells. Amount of protein was normalized to *β*-actin and is relative to amount in control cells. **(c)** Percentage of early and late apoptotic cells in uninfected and infected control RNAi-treated RAW 264.7 cells (ctrl-siRNA and ctrl-siRNA/ECTV, respectively) and in uninfected and infected RAW 264.7 cells after treatment with siRNA for *beclin 1* transcript (siBecn 1 and siBecn 1/ECTV, respectively). RAW 264.7 cells were transfected prior to ECTV-MOS infection and 18 hpi apoptosis was evaluated with the Annexin V-FITC apoptosis detection kit and flow cytometry. **(d)** Representative dot plots showing the percentage of early (Annexin V positive, PI negative) and late (Annexin V positive, PI positive) apoptotic cells. Numbers within quadrants represent the percentage of positive cells for a given marker. The values are presented as the mean ± SD from 4 independent experiments. Statistical significance is indicated by *asterisks* (Student's *t* test or Mann–Whitney U test, $*p < 0.05$, $**p < 0.01$).

infected siBecn 1 macrophages at 18 hpi with ECTV-MOS as compared to uninfected control and uninfected siBecn 1 cells, respectively (Fig. 4a and 4d). Moreover, at 18 hpi with ECTV-MOS a statistically significant ($p = 0.0307$) decrease in the percentage of late apoptotic/necrotic cells was observed in infected Beclin 1 siRNA-transfected RAW 264.7 cells compared to infected control macrophages (Fig. 4c and 4d). Our results suggest that Beclin 1 participates in regulation of apoptosis during the later stages of ECTV-MOS life cycle in RAW 264.7 macrophages.

Level of apoptosis in ECTV-MOS infected macrophages after pharmacological modulation of autophagy

To support our *beclin1* siRNA data, we pharmacologically modulated autophagy with wortmannin (inhibitor) or rapamycin (inductor). First, we established the corresponding concentrations of compounds, which on the one hand were not cytotoxic to macrophages, and on the other hand could modulate the process of autophagy (data not shown). After 2 h treatment of RAW 264.7 cells with 0.1 μg/mL of wortmannin, the LC3-II/*β*-actin ratio decreased compared to untreated cells, as shown by Western blot assay (Fig. 5a and 5b). Cells treated with 50 nM rapamycin for 30 min exhibited increased autophagosome formation as revealed by punctate MDC labeling (Fig. 5c).

After pharmacological treatment, macrophages were infected with ECTV-MOS and after 18 h the percentage of early and late apoptotic cells was quantified by Annexin V and propidium iodide (PI) staining and flow cytometry. The percentage of early apoptotic cells did not significantly change, neither in uninfected and infected RAW 264 cells nor uninfected and infected cells treated with pharmacological modulators of autophagy (Fig. 5d and 5e). However, statistically significant ($p = 0.0001$) increase in percentage of late apoptotic/necrotic cells was observed in all experimental culture systems exposed to ECTV-MOS compared to equivalent uninfected systems (Fig. 5d and 5e). Moreover, macrophages treated with rapamycin and infected with ECTV-MOS displayed significantly increased percentage of

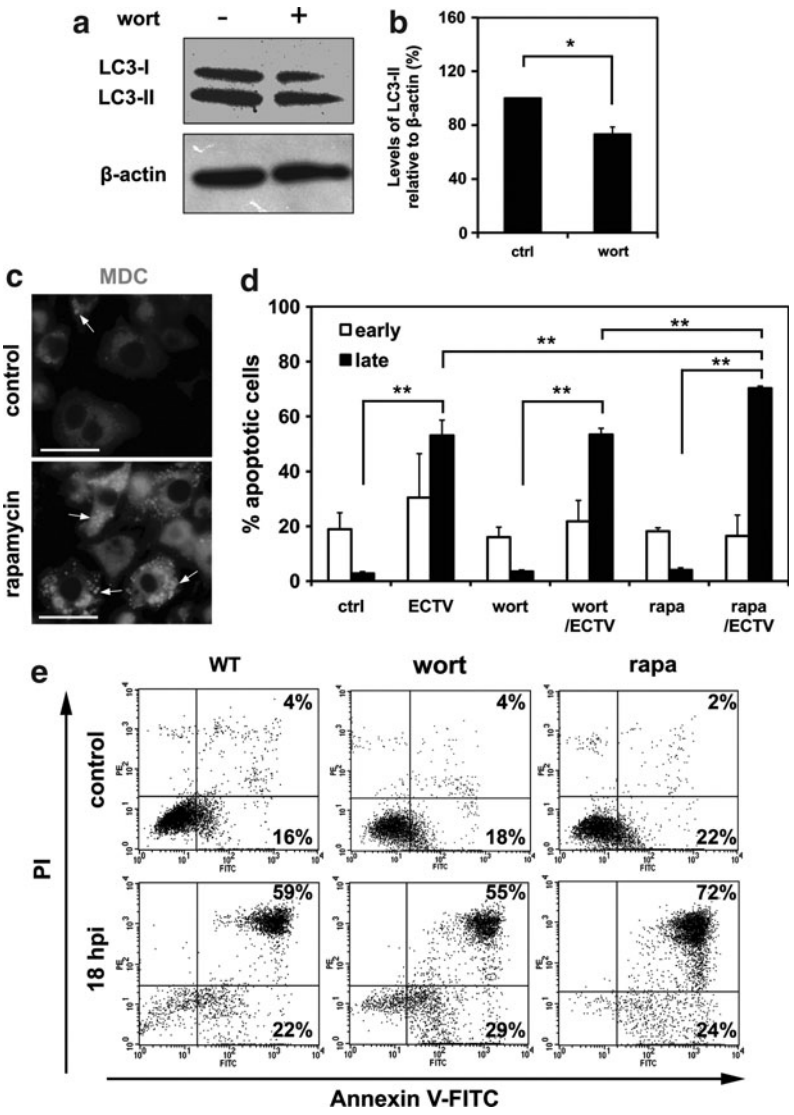

FIG. 5. Effects of wortmannin and rapamycin on ECTV-MOS-induced apoptosis in RAW 264.7 cells. **(a)** Western blot analysis of LC3-I (18 kDa) and LC3-II (16 kDa) expression in untreated WT cells and cells treated for 2 h with wortmannin at a final concentration of 0.1 μg/mL. The β-actin (42 kDa) was used as a loading control. **(b)** Quantitative analysis of LC3-II level in control WT cells and wortmannin-treated cells. Amount of protein was normalized to β-actin and is relative to amount in control cells. **(c)** Fluorescence microscopy detection of MDC-positive cytoplasmic structures (indicated by *arrows*) in untreated control cells and cells incubated for 30 min with 50 nM rapamycin. **(d)** The percentage of early and late apoptotic cells in mock- or ECTV-MOS-infected WT, wortmannin- or rapamycin-treated RAW 264.7 macrophages. Cells were incubated with pharmacological modulators of autophagy prior to ECTV-MOS infection and 18 hpi apoptosis was assessed using Annexin V-FITC apoptosis detection kit followed by flow cytometry. **(e)** Representative dot plots showing the percentage of early (Annexin V positive, PI negative) and late (Annexin V positive, PI positive) apoptotic cells. Numbers correspond to the percentage of positive cells in the given quadrant. The values are presented as the mean ± SD from 4 to 6 independent experiments. Statistically significant differences are indicated by *asterisks* (Student's *t* test or Mann–Whitney U test, $*p < 0.05$, $**p < 0.01$).

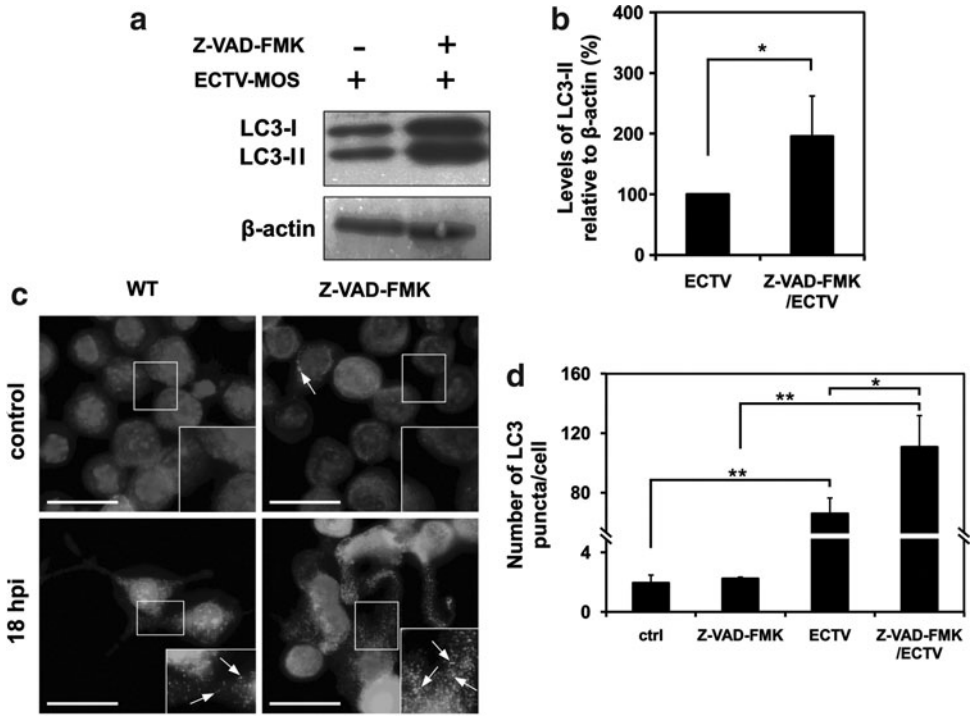

FIG. 6. Inhibition of apoptosis by Z-VAD-FMK increases the level of autophagy in ECTV-MOS-infected RAW 264.7 macrophages. RAW 264.7 cells were infected with ECTV-MOS and treated in parallel with 20 μM Z-VAD-FMK or left untreated. After 18 h of incubation, the expression of LC3 was analyzed by Western blot and fluorescence microscopy. **(a)** Western blot analysis of LC3-I (16 kDa) and LC3-II (18 kDa) expression in ECTV-MOS-infected WT and Z-VAD-FMK-treated cells. The β-actin (42 kDa) served as a loading control**. (b)** Quantitative analysis of LC3-II level in WT and Z-VAD-FMK-treated cells infected with ECTV-MOS. Amount of LC3-II was normalized to β-actin and is relative to amount in ECTV-MOS-infected WT cells. **(c)** Fluorescence microscopy analysis of LC3 expression in WT and Z-VAD-FMK-treated cells at 18 hpi with ECTV-MOS. Nuclear and viral DNA was stained with DAPI. LC3 aggregation is indicated by *arrows*. Scale bars: 30 μm. **(d)** Quantification of number of LC3 puncta per cell. The average number of LC3 puncta/cell was counted from > 100 cells per experimental condition. All results are the means ± SD from 3 independent experiments. Statistically significant differences are indicated by *asterisks* (Student's *t* test or Mann–Whitney U test, $*p < 0.05$, $**p < 0.01$).

late apoptotic/necrotic cells compared to infected untreated RAW 264.7 cells ($p = 0.0004$) or infected wortmannin-treated RAW 264.7 ($p = 0.0001$) macrophages (Fig. 5d and 5e). Results suggest that apoptosis induced during ECTV-MOS infection is partially regulated by autophagy/autophagic cell death.

Inhibition of apoptosis promotes autophagy is RAW 264.7 macrophages infected with ECTV-MOS

Our next question concerned the role of apoptosis in regulation of autophagy during ECTV-MOS replication. To block apoptosis we used Z-VAD-FMK, a commonly used caspase inhibitor. Infected RAW 264.7 macrophages treated with caspase inhibitor showed increased LC3-II/β-actin ratio compared to RAW 264.7 macrophages infected with ECTV-MOS only (Fig. 6a and 6b). Moreover, fluorescence microscopy analysis revealed enhanced formation of punctate aggregates of LC3 protein in ECTV-MOS-infected cells exposed to Z-VAD-FMK (Fig. 6c). Statistical analysis showed a significant increase in number of LC3 puncta per cell in group of infected WT cells compared to uninfected WT cells ($p = 0.0005$), infected Z-VAD-FMK-treated cells compared to uninfected Z-VAD-FMK-treated cells ($p = 0.0009$) and infected Z-VAD-FMK-treated cells compared to infected WT cells ($p = 0.0306$) (Fig. 6d). There were no significant differences in number of LC3 aggregates per cell between uninfected WT and Z-VAD-FMK-treated cells (Fig. 6d). Our data indicate that ectromelia virus infection increases autophagy in macrophages when apoptosis is inhibited.

Discussion

In addition to the physiological role of autophagy in providing nutrients during starvation period, autophagy also represents two opposing mechanisms by which cell death or cell survival can be induced. A problem in the explicit evaluation of autophagy arises from its dual role in the development of diseases (such as cancer, neurodegeneration, muscular disorder) and in the maintenance of homeostasis (1,33). Because autophagy is involved in a number of intracellular cell signaling pathways, it is extremely difficult to assess its role unambiguously in these two processes. Moreover, reliable methods for its evaluation are still under development.

In the present study, autophagy in ECTV-MOS-infected macrophages was analyzed quantitatively by densitomertic measurement of the ratio of LC3-II to β-actin bands obtained by Western blot assay. The LC3-II isoform binds to autophagosome membranes and its amount is positively correlated with the level of autophagosome formation (26). Western blot analysis of LC3 expression was supported by fluorescence microscopy assessment of LC3 distribution within the cell cytoplasm where LC3 was visualized as punctate structures representing autophagosomes (43). Moreover, we used additional methods such as MDC and Lysotracker staining to evaluate autophagy during ECTV-MOS replication in macrophages. Although MDC and Lysotracker have been shown to have higher affinity for lysosomes and cannot be used as a specific autophagosomes indicators (43), those dyes are still widely used as a complementary methods for autophagy monitoring (7,29,31,46).

As previously mentioned, initial *in vitro* studies focused on determination of autophagy extent in RAW 264.7 macrophages during the course of ECTV-MOS infection. ECTV-MOS is able to replicate productively in RAW 264.7 cells (Fig. 1). Autophagy was present in macrophages between 2–24 hpi as revealed by increased level of LC3-II protein (Fig. 2). Induction of autophagy was also confirmed by fluorescence microscopy, which revealed punctate aggregates of LC3 protein within cytoplasm of ECTV-MOS-infected cells what corresponds to the emerging autophagic vacuoles. Analysis using MDC or Lysotracker Red demonstrated the intensive formation of vesicles, presumably late stage or acidified autophagosomes (Fig. 3). This comprehensive picture shows a significant association of autophagy with ECTV-MOS infection in RAW 264.7 macrophages.

It is not known, however, whether autophagy plays a role in the protection of ECTV-MOS infected cells from death or contributes to their rapid apoptosis. Also, it is not clear whether autophagy participates in ECTV-MOS elimination or favors a rapid propagation of virus infection. Our preliminary studies aiming to clarify the role of autophagy during ECTV-MOS infection revealed that there is no relationship between autophagy and virus multiplication in culture cells. As determined by plaque assay, the virus titers for infected untreated or wortmannin-treated RAW 264.7 macrophages were similar (data not shown). This confirms results by Zhang and colleagues (59) that replication of VACV is not dependent on autophagic machinery. However, it is possible that the sensitivity of the plaque assay method was not sufficient enough to determine differences in ECTV-MOS life cycle dependent on autophagy and/or changes associated with autophagy inhibition did not affect the cytopathic properties of the virus.

Next, we analyzed the expression of a unique autophagy-related protein—Beclin 1 in ECTV-MOS-infected RAW 264.7 cells. Western blot assay did not reveal any changes in Beclin 1 levels between uninfected and ECTV-MOS-infected macrophages up to 24 hpi (Fig. 2). Meanwhile, fluorescent microscopy analysis demonstrated strong co-localization of Beclin 1 with extranuclear virus replication centers (Fig. 3b). Such distribution of Beclin 1 was also observed in ECTV-MOS-infected L929 fibroblasts (41), which may suggest that Beclin 1 plays an important role in efficient ECTV-MOS replication and/or survival in infected cells. It has been shown that the replication of human immunodeficiency virus type-1 (HIV-1) was reduced in primary cells with knockdown of Beclin 1, ATG5, or ATG7 expression with shRNA and/or siRNA (4,32). Moreover, we cannot exclude that such mobilization of Beclin 1 to ECTV-MOS replication centers prevents its interaction with anti-apoptotic proteins (e.g., Bcl-2), thereby stimulating the assembly of pre-autophagosomal structures that lead to autophagy (40). Our previous study showed that in the cytoplasm of ECTV-MOS-infected L929 fibroblasts there was a decrease in Bcl-2-Beclin 1 co-localization, especially within the viral replication sites (41). Our data suggest that ECTV-MOS may exploit a new, yet undefined, host response modifier (HRM) protein to regulate autophagy by interacting with Beclin 1.

Binding of Beclin 1 by many viruses, such as herpes simplex virus (HSV), Kaposi sarcoma-associated herpesvirus (KSHV) and murine herpesvirus 68 (MHV-68), inhibits autophagosome generation, which leads to enhancement of virus replication, virulence, and/or increases their persistence *in vivo* (44). Other viruses stabilize autophagosomes and prevent their fusion with lysosomes by targeting Beclin 1. Influenza virus and HIV target Beclin 1 and inhibit autophagolysosome formation presumably by stabilizing complexes of Beclin 1, Vps34, Vps15, UVRAG (UV irradiation resistance-associated gene), and Rubicon (RUN domain and cysteine-rich domain containing, Beclin 1-interacting protein) (44). Rubicon reduces Vps34 activity and arrests autophagosome maturation (60). Alternatively, some viruses usurp autophagy to enhance their efficient replication. Dreux and colleagues (11) demonstrated that autophagy proteins, such as Beclin 1, Atg4B, Atg5, and Atg12, were required for translation and/or delivery of incoming hepatitis C virus (HCV) RNA to the translation apparatus for initiation of virus replication. On the other hand, dengue virus (DENV) exploits autophagy for regulation of lipid metabolism to promote its efficient replication (19).

As we mentioned before, induction of autophagy may contribute to cell survival or death during apoptosis. To determine the crosstalk between autophagy and apoptosis in RAW 264.7 macrophages during ECTV-MOS infection, we modulated the autophagic pathway prior to infection with the virus. Because Beclin 1 regulates both processes (10,27) and its clear contribution is observed during ECTV-MOS infection, we investigated the level of apoptosis in RAW 264.7 cells transfected with *beclin 1* siRNA prior to infection. Knockdown of *beclin 1* did not affect the percentage of early apoptotic cells during ECTV-MOS infection (Fig. 4b and 4c). However, we observed a decrease in the percentage of late apoptotic cells in ECTV-MOS-infected macrophages transfected with *beclin 1* siRNA compared to infected control siRNA cells (Fig. 4b and 4c). Our previous investigation showed similar results in infected L929 cells with knockdown of *beclin 1*. ECTV-MOS-infected siBecn 1 fibroblasts exhibited a decrease in early and late apoptosis compared to infected control cells (41). These results suggest that Beclin 1 is involved in the death execution process during ECTV-MOS infection.

Beclin 1 is a regulator of crosstalk between autophagy and apoptosis. In relation to apoptosis, Beclin 1 may act as a pro- or anti-apoptotic protein (27,55). Wirawan and colleagues (55) showed that Beclin 1 can acquire an apoptosis-promoting function through its cleavage by several caspases. Caspase-mediated cleavage of Beclin 1, in response to different

inducers of the intrinsic or extrinsic pathways of apoptosis, results in generation of Beclin 1 C- and N-terminal fragments. Beclin 1-C translocates from the cytosol to mitochondria and induces the release of pro-apoptotic factors, suggesting a mechanism by which Beclin 1-C may favor apoptosis (55). On the contrary, Beclin 1 functions as an anti-apoptotic protein in several settings, such as chemotherapy, irradiation, immunotherapy, nutrient deprivation, angiogenesis inhibitors, and hypoxia. The precise mechanism of apoptosis inhibition by Beclin 1 has not been clearly demonstrated. However, it may be associated with unregulated autophagy acting as an anti-injury mechanism, responsible for removing of apoptotic cells (27).

Subsequently, we analyzed early and late apoptosis in ECTV-MOS infected RAW 264.7 cells during pharmacological manipulation of autophagy using wortmannin (inhibitor) or rapamycin (inductor). Wortmannin is an inhibitor of PI3K, which blocks autophagy at the early stage (12). Rapamycin inhibits cell cycle progression by blocking the mTOR kinases through formation of complexes with the FKBP12 propyl isomerase (16,48). Blockade of mTOR leads to dephosphorylation of ULK1, ULK2 (two Atg1 homologues), and Atg13 and activates ULK to phosphorylate a focal adhesion kinase family-interacting protein of 200 kDa (FIP200) (24,25). During early stages of apoptosis, cells lose their normal phospholipid asymmetry in the plasma membrane, which results in phosphatidylserine (PS) exposition in the exoplasmic leaflet. Early apoptotic cells still maintain membrane integrity, whereas late apoptotic cells lose plasma membrane integrity. Interestingly, our results indicated that inhibition of autophagy by wortmannin did not influence the percentage of early and late apoptotic cells in infected RAW 264.7 macrophages (Fig. 5). It suggests that during ECTV-MOS infection the inhibition of autophagy at its early stage does not affect induction of apoptosis in RAW 264.7 cells. It is not excluded that apoptosis may be differentially regulated in ECTV-MOS infected cells depending on the stage and the type of autophagic pathway, which is inhibited. Recently, Xi and colleagues (56) have demonstrated that inhibition of autophagy at the autophagosome formation stage and autophagy execution stage decreased the apoptosis induced by enterovirus 71 (EV71). However, inhibition of autophagy at the stage of autophagosome and lysosome fusion promoted the EV71-induced apoptosis (56). Our studies revealed that induction of autophagy by rapamycin increased the level of late apoptotic/necrotic cells (Fig. 5), suggesting that enhancement of autophagy significantly affects the induction of apoptosis in this system. It may suggest that apoptosis induced in ECTV-MOS-infected RAW 264.7 macrophages is partially dependent on autophagy/autophagic cell death and, presumably, is regulated by a common mechanism.

Cooperative relationship between autophagy and apoptosis was shown in several investigations. For example, cell-expressed HIV-1 envelope glycoproteins (Env) induced autophagy in uninfected $CD4^+$ T lymphocytes by binding to CXCR4. Blockade of autophagy by treatment with drugs [3-methyladenine (3-MA) and bafilomycin A1] or by the siRNA knockdown of *beclin 1* or *atg7* resulted in dramatic decrease of caspase-3 activity and totally inhibited Env-mediated cell death (15). Similar results were obtained in oxidative stress-mediated cell death in photoreceptors in *in vitro* and *in vivo* model studies (31). Treatment of 661W photoreceptor cells with either 3-MA or siRNA for *atg5* and *beclin 1* partially blocked H_2O_2-induced cell death (31). Those studies clearly prove that under certain environmental conditions autophagy may participate in cell death execution, possibly through apoptosis or initiation of apoptosis. On the contrary, it was shown that inhibition of autophagy in MEFs (by Atg5 deletion) increased apoptosis induced by influenza virus, whereas permitting autophagy to progress (by M2 deletion) decreased apoptosis induced by influenza virus (17). Similarly, Chikungunya virus (CHIKV)-induced autophagy delayed apoptotic cell death in MEFs, whereas silencing of autophagy genes resulted in increased apoptotic cell death, enhancing propagation of virus in cultured cells (23).

Our next question concerned the effect of apoptosis inhibition on autophagy level in ECTV-MOS-infected RAW 264.7 cells. Apoptosis was blocked by Z-VAD-FMK, which irreversibly binds to the catalytic site of a wide spectrum of active caspases and forms a covalent inhibitor/enzyme complex. Our results indicated that Z-VAD-FMK treatment increased LC3-II expression and punctate accumulation in cells infected with ECTV-MOS (Fig. 6), suggesting that autophagy increases when apoptotic cell death pathways are blocked. It is not excluded that during ECTV-MOS infection in RAW 264.7 macrophages autophagy could potentially provide an alternative pathway of cell death when apoptosis is inhibited. On the other hand, Z-VAD-FMK was shown to block the clearance of autophagosome materials and to impair autophagic flux (20). Inhibition of cathepsins (47) and calpain (53) was observed, however, in cells treated with high concentrations (100 μM) of Z-VAD-FMK. Our results did not demonstrate the increase in LC3 aggregates in RAW 264.7 macrophages treated with Z-VAD-FMK (Fig. 6). Moreover, in our experiments Z-VAD-FMK was used at much lower concentration (20 μM) and potential inhibition of cathepsins and calpain activity was unlikely to have a major impact on the results (37).

Several studies have demonstrated that autophagy may be used as a killing mechanism during blockade of apoptosis. For example, autophagic cell death in L929 fibroblasts was induced by caspase-8 inhibition and required two autophagy related genes, *atg7* and *beclin 1* (58). Blockade of caspase-8 triggered cell death pathway through activation of the receptor-interacting protein and c-Jun amino-terminal kinase (58). Further, autophagic cell death was activated in apoptosis-resistant Bax/Bak double knockout MEFs treated with etoposide or staurosporine (50). Inhibition of autophagy gens, *atg5* and *beclin 1* increased viability of $bax^{-/-}$ and $bak^{-/-}$ MEFs after death stimulation (50). Similarly, autophagy contributed to the execution of cell death in macrophages treated with lipopolysaccharides (LPSs) and the caspase inhibitor Z-VAD (57). Inhibition of autophagy either by *beclin 1* RNAi or by chemical inhibitors resulted in a blockade of caspase-independent macrophage cell death (57). All studies described above clearly show that autophagy and apoptosis share common regulatory mechanisms and both may act to eliminate the cell.

Interestingly, under some circumstances, autophagy may enable the apoptotic program by participating in formation of certain apoptotic morphological changes, without leading to death itself (13). For example, formation of autophagic

vesicles together with membrane blebbing and partial nuclear condensation occurred in a caspase independent manner (22). Those morphological events were mediated by pro-apoptotic calcium/calmodulin-regulated Ser/Thr death kinases: DAPk (death-associated protein kinase) and DRP-1 (DAPk-related protein kinase 1) (22). Furthermore, an essential role of autophagy genes in promoting the engulfment and clearance of apoptotic bodies by phagocytes was observed during mouse embryonic development *in vivo* and in the *in vitro* embryoid bodies (EBs) model (45). Generation of "eat-me" signal of phosphatidylserine (PS) exposure on the outer membrane and secretion of "come-get-me" signal through release of lysophosphatidylcholine (LPC) were severely impaired in *atg5*$^{-/-}$ and *beclin 1*$^{-/-}$ EBs. Presumably, defects in engulfment of apoptotic cell, exposure of PS, and secretion of LPC were associated with the lack of autophagy-dependent ATP production in autophagy null EBs (45).

It should be noted that the high level of autophagy detected in RAW 264.7 cells during replication of ECTV-MOS may be related to phagocytic activity and/or antigen presentation capabilities of macrophages. It is well known that autophagy is implicated in major histocompatibility complex (MHC) class I and MHC class II antigen presentation (8,35), and is a possible mechanism responsible for the MHC class I-mediated cross-presentation of exogenous tumor (18) or viral (14) antigens. For example, during HSV-1 infection of human macrophages autophagy facilitated the late processing of exogenous viral proteins, their presentation on MHC class I molecules, and stimulation of $CD8^+$ T cells (14), which are critical for protective immune response against viruses.

In conclusion, we have shown for the first time that autophagy is induced in macrophages during ECTV-MOS infection *in vitro*. During later stages of infection, autophagy may occur concurrently with apoptosis in RAW-264.7 cells and participate partially in the demise of macrophages possibly by apoptosis. Additionally, when apoptosis is inhibited, autophagy likely contributes to the execution of cell death in infected RAW 264.7 macrophages. We conclude that autophagy is an important mechanism that regulates ECTV-MOS replication in cultured cells. However, autophagy is involved in many biological functions, therefore, the exact role of this process during ectromelia virus infection needs to be clarified in future studies. These findings may ultimately contribute to harness apoptotic and autophagic pathways as novel targets for antiviral therapy.

Acknowledgments

We thank Felix N. Toka (Ph.D. from the WULS-SGGW) for critical reading of the manuscript. This work was supported by Grant No. 2 PO5A 050 30 from the Ministry of Science and Higher Education in Warsaw (to MN) and by Mazovia PhD Scholarship 2009 No. 0853/3 (to LM) co-financed from the European Social Fund and Polish state budget.

Author Disclosure Statement

No competing financial interests exist.

References

1. Baehrecke EH: Autophagy: Dual roles in life and death? Nat Rev Mol Cell Biol 2005;6:505–510.
2. Bhutia SK, Dash R, Das SK, *et al.* Mechanism of autophagy to apoptosis switch triggered in prostate cancer cells by antitumor cytokine *mda*-7/IL-24. Cancer Res 2010;70:3667–3676.
3. Boratyńska A, Martyniszyn L, Szulc L, Krzyżowska M, Szczepanowska J, and Niemiałtowski MG: Contribution of rearranged actin structures to the spread of Ectromelia virus infection *in vitro*. Acta Virol 2010;54:41–48.
4. Campbell GR, and Spector SA: Hormonally active vitamin D3 (1α,25-dihydroxycholecalciferol) triggers autophagy in human macrophages that inhibits HIV-1 infection. J Biol Chem 2011;286:18890–18902.
5. Chaudhri G, Panchanathan V, Buller RML, *et al.* Polarized type 1 cytokine response and cell-mediated immunity determine genetic resistance to mousepox. Proc Natl Acad Sci USA 2004;101:9057–9062.
6. Cheng Y, Ren X, Zhang Y, *et al.* eEF-2 kinase dictates cross-talk between autophagy and apoptosis induced by Akt inhibition, thereby modulating cytotoxicity of novel Akt inhibitor MK-2206. Cancer Res 2011;71:2654–2663.
7. Chu CT, Plowey ED, Dagda RK, Hickey RW, Cherra III SJ, and Clark RSB: Autophagy in neurite injury and neurodegeneration: *in vitro* and *in vivo* models. Methods Enzymol 2009;453:217–249.
8. Crotzer VL, and Blum JS: Autophagy and its role in MHC-mediated antigen presentation. J Immunol 2009;182:3335–3341.
9. Cymerys J, Krzyżowska M, Spohr I, Winnicka A, and Niemiałtowski M: Hsp-27, hsp-70 and hsp-90 expression and apoptosis in macrophages during ectromelia (mousepox) virus infection. Centr Eur J Immunol 2009;34:20–28.
10. Djavaheri-Mergny M, Maiuri MC, and Kroemer G: Cross talk between apoptosis and autophagy by caspase-mediated cleavage of Beclin 1. Oncogene 2010;29:1717–1719.
11. Dreux M, Gastaminza P, Wieland SF, and Chisari FV: The autophagy machinery is required to initiate hepatitis C virus replication. PNAS 2009;106:14046–14051.
12. Dunn SR, Schnitzler CE, and Weis VM: Apoptosis and autophagy as mechanisms of dinoflagellate symbiont release during cnidarian bleaching: Every which way you lose. Proc R Soc B 2007;274:3079–3085.
13. Eisenberg-Lerner A, Bialik S, Simon H-U, and Kimchi A: Life and death partners: Apoptosis, autophagy and the cross-talk between them. Cell Death Differ 2009;16:966–975.
14. English L, Chemali M, Duron J, *et al.* Autophagy enhances the presentation of endogenous viral antigens on MHC class I molecules during HSV-1 infection. Nat Immunol 2009;10:480–487.
15. Espert L, Denizot M, Grimaldi M, *et al.* Autophagy is involved in T cell death after binding of HIV-1 envelope proteins to CXCR4. J Clin Invest 2006;116:2161–2172.
16. Fingar DC, Richardson CJ, Tee AR, Cheatham L, Tsou C, and Blenis J: mTOR controls cell cycle progression through its cell growth effectors S6K1 and 4E-BP1/eukaryotic translation initiation factor 4E. Mol Cell Biol 2004;24:200–216.
17. Gannagé M, Dormann D, Albrecht R, *et al.* Matrix protein 2 of influenza A virus blocks autophagosome fusion with lysosomes. Cell Host Microbe 2009;22:367–380.
18. Hanaf L-A, Leclerc D, and Lapointe R: Autophagy is implicated in MHC class I antigen cross-presentation mediated by potexvirus VLP. J Immunol 2012;188:106.10.
19. Heaton NS, and Randall G: Dengue virus induced autophagy regulates lipid metabolism. Cell Host Microbe 2010;8:422–432.

20. Herzog C, Yang C, Holmes A, and Kaushal GP: zVAD-fmk prevents cisplatin-induced cleavage of autophagy proteins but impairs autophagic flux and worsens renal function. Am J Physiol Renal Physiol 2012;303:F1239–1250.
21. Høyer-Hansen M, Bastholm L, Szyniarowski P, *et al.* Control of macroautophagy by calcium, calmodulin-dependent kinase kinase-β, and Bcl-2. Mol Cell 2007;25:193–205.
22. Inbal B, Bialik S, Sabanay I, Shani G, and Kimchi A: DAP kinase and DRP-1 mediate membrane blebbing and the formation of autophagic vesicles during programmed cell death. J Cell Biol 2002;157:455–468.
23. Joubert PE, Werneke SW, de la Calle C, *et al.* Chikungunya virus-induced autophagy delays caspase-dependent cell death. J Exp Med 2012;209:1029–1047.
24. Jung CH, Jun CB, Ro SH, *et al.* ULK-Atg13-FIP200 complexes mediate mTOR signaling to the autophagy machinery. Mol Biol Cell 2009;20:1992–2003.
25. Jung CH, Ro SH, Cao J, Otto NM, and Kim DH: mTOR regulation of autophagy. FEBS Lett 2010;584:1287–1295.
26. Kabeya Y, Mizushima N, Ueno T, *et al.* LC3, a mammalian homologue of yeast Apg8p, is localized in autophagosome membranes after processing. EMBO J 2000;19:5720–5728.
27. Kang R, Zeh HJ, Lotze MT, and Tang D: The Beclin 1 network regulates autophagy and apoptosis. Cell Death Differ 2011;18:571–580.
28. Kihara A, Kabeya Y, Ohsumi Y, and Yoshimori T: Beclin-phosphatidylinositol 3-kinase complex functions at the trans-Golgi network. EMBO Rep 2001;2:330–335.
29. Koga H, Kaushik S, and Cuervo AM: Altered lipid content inhibits autophagic vesicular fusion. FASEB J 2010;24:3052–3065.
30. Krzyżowska M, Schollenberger A, Skierski J, and Niemiałtowski M: Apoptosis during ectromelia orthopoxvirus infection is DEVDase dependent: In vitro and in vivo studies. Microbes Infect 2002;4:599–611.
31. Kunchithapautham K, and Rohrer B: Apoptosis and autophagy in photoreceptors exposed to oxidative stress. Autophagy 2007;3:433–441.
32. Kyei GB, Dinkins C, Davis AS, *et al.* Autophagy pathway intersects with HIV-1 biosynthesis and regulates viral yields in macrophages. J Cell Biol 2009;186:255–268.
33. Levine B, and Kroemer G: Autophagy in the pathogenesis of disease. Cell 2008;132:27–42.
34. Levine B, and Yuan J: Autophagy in cell death: An innocent convict? J Clin Invest 2005;115:2679–2688.
35. Li Y, Wang LX, Yang G, Hao F, Urba WJ, and Hu HM: Efficient cross-presentation depends on autophagy in tumor cells. Cancer Res 2008;6889–6895.
36. Liu Z, Lv YJ, Song YP, Li XH, Du YN, Wang CH, and Hu LK: Lysosomal membrane protein TMEM192 deficiency triggers crosstalk between autophagy and apoptosis in HepG2 hepatoma cells. Oncol Rep 2012;28:985–991.
37. Luo S, and Rubinsztein DC: Apoptosis blocks Beclin 1-dependent autophagosome synthesis—An effect rescued by Bcl-xL. Cell Death Differ 2010;17:268–277.
38. Lynn H, Horsington J, Ter LK, *et al.* Loss of cytoskeletal transport during egress critically attenuates ectromelia virus infection in vivo. J Virol 2012;86:7427–7443.
39. Maiuri MC, Zalckvar E, Kimchi A, and Kroemer G: Self-eating and self-killing: Crosstalk between autophagy and apoptosis. Nat Rev Mol Cell Biol 2007;8:741–752.
40. Marquez RT, and Xu L: Bcl-2:Beclin 1 complex: Multiple, mechanisms regulating autophagy/apoptosis toggle switch. Am J Cancer Res 2012;2:214–221.
41. Martyniszyn L, Szulc L, Boratyńska A, and Niemiałtowski MG: Beclin 1 is involved in regulation of apoptosis and autophagy during replication of ectromelia virus in permissive L929 cells. Arch Immunol Ther Exp 2011;59:463–471.
42. Martyniszyn L, Szulc-Dąbrowska L, Boratyńska-Jasińska A, Badowska-Kozakiewicz AM, and Niemiałtowski MG: *In vivo* induction of autophagy in splenocytes of C57BL/6 and BALB/c mice infected with ectromelia orthopoxvirus. Pol J Vet Sci 2013;16:25–32.
43. Mizushima N, Yoshimorim T, and Levine B: Methods in mammalian autophagy research. Cell 2010;140:313–326.
44. Münz C: Beclin-1 targeting for viral immune escape. Viruses 2011;3:1166–1178.
45. Qu X, Zou Z, Sun Q, Luby-Phelps K, Cheng P, Hogan RN, Gilpin C, and Levine B: Autophagy gene-dependent clearance of apoptotic cells during embryonic development. Cell 2007;128:931–946.
46. Raben N, Shea L, Hill V, and Plotz P: Monitoring autophagy in lysosomal storage disorders. Methods Enzymol 2009;453:417–449.
47. Rozman-Pungercar J, Kopitar-Jerala N, Bogyo M, *et al.* Inhibition of papain-like cysteine proteases and legumain by caspase-specific inhibitors: When reaction mechanism is more important than specificity. Cell Death Differ 2003;10:881–888.
48. Sabatini DM, Erdjument-Bromage H, Lui M, Tempst P, and Snyder SH: RAFT1: A mammalian protein that binds to FKBP12 in a rapamycin-dependent fashion and is homologous to yeast TORs. Cell 1994;78:35–43.
49. Scherz-Shouval R, Shvets E, Fass E, Shorer H, Gil L, and Elazar Z: Reactive oxygen species are essential for autophagy and specifically regulate the activity of Atg4. EMBO J 2007;26:1749–1760.
50. Shimizu S, Kanaseki T, Mizushima N, Mizuta T, Arakawa-Kobayashi S, Thompson CB, and Tsujimoto Y: Role of Bcl-2 family proteins in a non-apoptotic programmed cell death dependent on autophagy genes. Nat Cell Biol 2004;6:1221–1228.
51. Vousden KH, and Lane DP: p53 in health and disease. Nat Rev Mol Cell Biol 2007;8:275–283.
52. Wagner EK, Hewlett MJ, Bloom DC, and Camerini D: Replicating and measuring biological activity of viruses. In: *Basic Virology*, 3rd ed. Blackwell Publishing, Malden, 2008, pp. 155–172.
53. Waterhouse NJ, Finucane DM, Green DR, *et al.* Calpain activation is upstream of caspases in radiation-induced apoptosis. Cell Death Differ 1998;5:1051–1061.
54. Weidberg H, Shvets E, Shpilka T, Shimron F, Shinder V, and Elazar Z: LC3 and GATE-16/GABARAP subfamilies are both essential yet act differently in autophagosome biogenesis. EMBO J 2010;29:1792–1802.
55. Wirawan E, Walle LV, Vande L, *et al.* Caspase-mediated cleavage of Beclin-1 inactivates Beclin-1-induced autophagy and enhances apoptosis by promoting the release of proapoptotic factors from mitochondria. Cell Death Dis 2010;1:e18.
56. Xi X, Zhang X, Wang B, *et al.* The interplays between autophagy and apoptosis induced by enterovirus 71. PLoS ONE 2013;8:e56966.
57. Xu Y, Kim SO, Li Y, and Han J: Autophagy contributes to caspase-independent macrophage cell death. J Biol Chem 2006;281:19179–19187.
58. Yu L, Alva A, Su H, Dutt P, Freundt E, Welsh S, Baehrecke EH, and Lenardo MJ: Regulation of an *ATG7-beclin 1*

program of autophagic cell death by caspase-8. Science 2004; 304:1500–1502.
59. Zhang H, Monken CE, Zhang Y, Lenard J, Mizushima N, Lattime EC, and Jin S: Cellular autophagy machinery is not required for vaccinia virus replication and maturation. Autophagy 2006;2:91–95.
60. Zhong Y, Wang QJ, Jun Q, *et al.* Distinct regulation of autophagic activity by Atg14L and Rubicon associated with Beclin 1- phosphatidylinositol 3-kinase complex. Nat Cell Biol 2009;11:468–476.

Address correspondence to:
Dr. Marek Niemiałtowski
Division of Immunology
Department of Preclinical Sciences
Faculty of Veterinary Medicine
Warsaw University of Life Sciences-SGGW
Ciszewskiego Str. 8
02-786 Warsaw
Poland

E-mail: marek_niemialtowski@sggw.pl